

Systematic Strategy for Designing Imidazolium Containing Precursors To Produce *N*-Heterocyclic Carbenes: A DFT Study

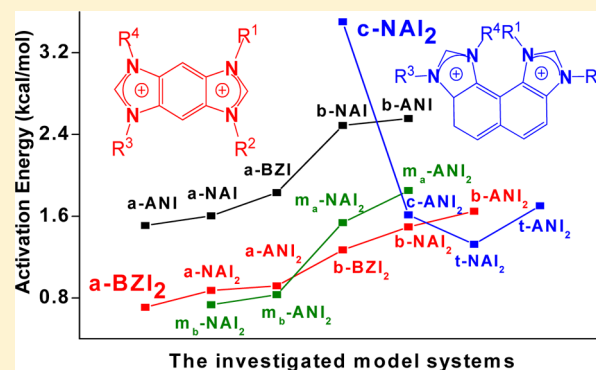
Kyung Yup Baek,[†] Ji Hye Jo,[†] Jong Hun Moon,[†] Juyoung Yoon,^{*,‡} and Jin Yong Lee^{*,†}

[†]Department of Chemistry, Sungkyunkwan University, Suwon 440-746, Korea

[‡]Department of Chemistry, Ewha Womans University, Seoul 120-750, Korea

S Supporting Information

ABSTRACT: A series of cationic *N*-heterocyclic carbene (NHC) precursors that can be utilized as fluorescent chemosensors for carbon dioxide capture were investigated by density functional theory (DFT) calculations. Activation energy barriers for the reactions of the cationic NHC precursors and hydrogen carbonate (HCO_3^-) based on intrinsic reaction coordinate (IRC) profiles as well as proton affinity of the precursors were compared. The calculated proton affinity of 1-ethyl-3-methylimidazol-2-ylidene was in good agreement with experimental one within the margin of error. We clarified main factors to lower the activation energy barrier based on the correlation among the number of *N*-heterocyclic functional group, aromatic ring size, and structural characteristics for the candidate compounds. On the basis of the results, it was verified that some of our model systems spontaneously generate NHCs without any specific catalyst.



INTRODUCTION

Since Buchner and Curtius (1885) found that carbene exists,¹ the species has been considered impossible to be isolated for tremendous reactivity until Igau et al. (1988) successfully synthesized stable five membered ring carbene including heteroatom.^{2,3} Thereafter, *N*-heterocyclic carbenes (NHCs) have been one of the most interesting chemical species for their versatile applicability in organic chemistry^{4–10} and have been utilized as organocatalysts and ligands for transition metals in many applied chemistry fields.^{11–15}

In particular, many chemists in green research fields have been interested in imidazolium salts (IMs) as precursors of stable NHCs, which not only act as chemosensors^{16–19} but also play an important role in carbon dioxide capture and utilization.^{20–23} Accordingly, their electronic and physical properties have been intensively studied with structural modifications, so-called substitution of functional groups attached to *N*-hetero atoms.^{24–30} However, there is lack of study for synthetic strategy pursuing efficient NHC precursors based on systematic investigation.

In previous work,¹⁶ we developed a fluorescent sensor utilizing tetrapropyl benzobisimidazolium (TBBI) salt with fluoride anion (F^-) and described the merit of the sensor in detail. It is noteworthy that fluoride anion caused barrierless process when generating free carbene. Because activation energy barrier is a criterion to distinguish the easiness of reaction, we employed herein hydrogen carbonate anion (HCO_3^-) instead of fluoride anion to discriminate the imidazolium-based NHC precursors by activation barrier.

Fluoride anion cannot give us which precursor will be better to generate NHC because it can produce NHC from the precursors without barrier similar to leveling effect in acidity strength.

To the best of our knowledge, not much is known in literature about correlation among the number of linker groups, aromatic ring size, and steric hindrance for precursors of NHCs. Our research purpose in this study is to establish their correlation and then find out main factor to lower activation energy barrier on the reaction of NHC precursors to produce NHCs. Lowering the barrier is important to make free carbene easily.

MODEL SYSTEMS

Figure 1 shows the imidazolium-based derivatives investigated in this work. For the candidates, we considered how effective they are as precursors of NHCs that can be utilized as carbon dioxide capture or chemosensor and noted their conformation dependence. In line with this, we devised three categories to find the dependence as the following: (1) Extending aromatic ring size, (2) increasing the number of imidazolium, namely, *N*-heterocyclic functional group, and (3) shifting the position of the imidazolium in the model systems. All substituents (R^1 , R^2 , R^3 , and R^4) attached to imidazolium moieties were replaced with methyl groups.

Received: December 20, 2014

Published: January 16, 2015

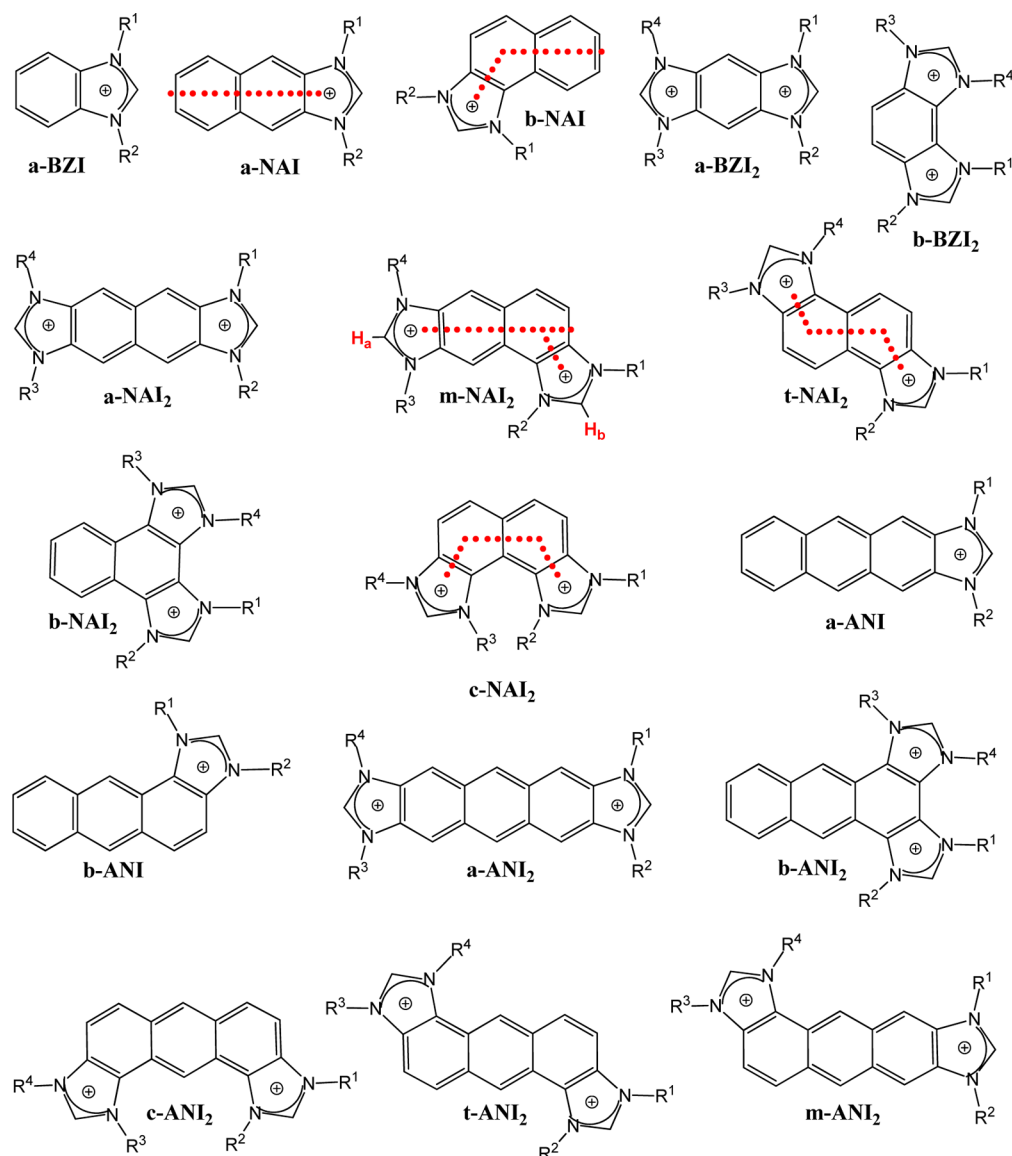


Figure 1. Molecular structures for the investigated *N*-heterocyclic carbene (NHC) precursors. “BZ”, “NA”, “AN”, and “I” denote benzene, naphthalene, anthracene, and methyl-substituent imidazolium, respectively. a-, b-, and m- are used in order to indicate different position of the imidazolium(s): a- for linear, b- for bent, and m- for mixed form. c-, and t- denote *cis*- and *trans*-isomer.

As a matter of convenience, we adopted the following notations for aromatic moiety and the number of the imidazolium when expressing each name of the model systems; BZI stands for 1,3-dimethyl-1*H*-benzimidazol-3-ium, “a-” and “b-” denote the linear and bent form, respectively, considering the imidazolium ring and naphthalene or anthracene ring direction as seen in Figure 1. In addition, NAI₂ and ANI₂ have mixed form of linear and bent arrangement as well as *cis* and *trans* form, which are denoted as “m-”, “c-”, and “t-” notations, respectively.

■ COMPUTATIONAL DETAILS

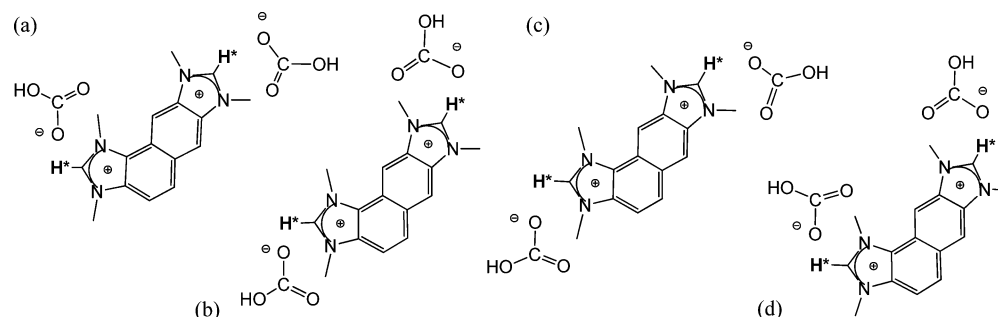
It is important to determine appropriate theoretical method to meet the purpose of calculations. The most widely used hybrid functional B3LYP^{31–33} in DFT calculations gives considerable underestimated energy for noncovalent interaction systems^{34–36} and π -conjugated systems,³⁷ whereas M06-2X functional developed by Truhlar et al. gives good performance not only for them but for thermochemical kinetic calculations: hydrogen-transfer barrier height, proton affinity (PA), atomic energy (AE), electron affinity (EA), and ionization

potential (IP) when applying for conjugated π systems and hydrocarbons.³⁸ Hence, for the versatility of NHCs considered, it is worth doing systematic investigation on their precursors using M06-2X functional.

In this work, all calculations were performed with a suite of Gaussian09 programs.³⁹ We accomplished geometry optimization for each species employing M06-2X^{38,39} functional with the standard 6-311+G(d,p) basis set: mono- and bis-imidazolium derivatives (cation), deprotonated mono- and bis-imidazolium derivatives (neutral), and hydrogen carbonate (anion), respectively. Basically, the charge of EMI, BZI, NAI, and ANI is +1, and that of BZI₂, NAI₂, and ANI₂ is +2.

For the spin multiplicity of carbene ($\text{H}_2\text{C}:$) and its derivatives ($\text{R}_2\text{C}:$), there are two possibilities: singlet or triplet. In this work, it was clarified that all the deprotonated species, carbenes, have a singlet ground state through the comparison of their energies with the corresponding triplet states. In other words, all the carbenes in the triplet ground state were higher in energy by 45–80 kcal/mol than the corresponding singlet states. Therefore, we herein only analyzed the results on the singlet calculations.

Each proton affinity for the molecules was estimated from the energy gap between carbene form (neutral) and their protonated form

Scheme 1. Various Orientations between Bis-Imidazolium and Hydrogen Carbonates^a

^aHere, asterisk represents deprotonated site to generate carbene.

(cation) with thermal energy correction. In order to estimate activation energies of NHC precursors, we initially set HCO_3^- around the active sites of imidazolium moieties to generate carbene as shown in Scheme 1 and conducted geometry optimization for the reactant. In sequence, we investigated intrinsic reaction coordinate (IRC)³⁹ calculations in order to find the optimized structure in the corresponding transition state (TS) for the most probable reaction path between reactant and product. We also carried out polarizable continuum model (PCM) calculations for more realistic description of ionic species.

RESULTS AND DISCUSSION

Proton affinity (PA) is used to measure gas-phase basicity of molecule and it is defined as exoergic energy when a system accepts one extra proton: $\text{PA} = E(\text{MH}^+) - E(\text{M}) - E(\text{H}^+)$, where $\text{M} = \text{EMI}, \text{BZI}, \text{NAI}, \text{ANI}, \text{BZI}_2, \text{NAI}_2,$ and ANI_2 . The electronic energy of a proton is 0, that is, $E(\text{H}^+) = 0$. PA value is directly proportional to basicity and it has strong influence on stability of cationic NHC precursors.⁴⁰ It means that the cationic NHC precursors are more stable as their PA increase, whereas it is hard to generate their neutral carbenes.

To the best of our knowledge, there is little literature on experimental PA for the NHCs shown in Figure 1. Lee et al. reported experimental PA of 1-ethyl-3-methylimidazol-2-ylidene (EMI).²⁹ We obtained its theoretical PA value and compared with the experimental value in order to verify the reliability of computational method used in this work. As seen in Table 1, the estimated PA value by M06-2X gives good agreement with experimental one within the margin of error.

On the basis of their PA values, we investigated the possibility of deprotonation for other sites of a-BZI before full-scale discussion on our results for NHC precursors: 288.8 kcal/mol for the methyl group, 296.1 kcal/mol for H_1 of the benzene ring, and 312.8 kcal/mol for H_2 of the benzene ring, respectively. It means that imidazolium moiety is prominent to the other groups as an active site to generate carbene.

In Table 1, PA values among a-type monoimidazolium candidates are almost equivalent regardless of their aromatic ring size as well as their bis-imidazolium ones. However, those of b-type imidazolium model systems show discrepancies: 1.7 kcal/mol between b-NAI and b-ANI, within 2.8 kcal/mol among b-type bisimidazolium derivatives. The PA gaps between a- and b-types are considerable: 2.9 kcal/mol between a-NAI and b-NAI, and 4.3 kcal/mol between a-ANI and b-ANI.

Furthermore, for mixed types consisting of linear and bent arrangement, their PAs are considerably different depending on the deprotonation site: the discrepancy of 5.7 kcal/mol between $\text{m}_a\text{-ANI}_2$ and $\text{m}_b\text{-ANI}_2$. Here, the prefix m_a/m_b denotes the first deprotonation at linear/bent imidazolium

Table 1. Negative Proton Affinities (–PA) for the Corresponding NHCs of Model Systems^a

authentic sample, 1-ethyl-3-methylimidazol-2-ylidene (EMI)			
M06-2X ^b	experiment ^c	B3LYP ^d	CBS-QB3 ^d
258.5	254.0–260.6	261.4	264.5
imidazolium-based materials ^b			
compound	M06-2X	compound	M06-2X
a-BZI	255.7	b-NAI ₂	257.9
a-NAI	255.7	b-ANI ₂	259.1
a-ANI	256.0	$\text{m}_a\text{-NAI}_2$	255.8
b-NAI	258.6	$\text{m}_a\text{-ANI}_2$	255.9
b-ANI	260.3	$\text{m}_b\text{-NAI}_2$	259.9
		$\text{m}_b\text{-ANI}_2$	261.6
a-BZI ₂	257.6	c-NAI ₂	258.7
a-NAI ₂	257.3	c-ANI ₂	259.8
a-ANI ₂	257.3	t-NAI ₂	258.8
b-BZI ₂	256.3	t-ANI ₂	260.3

^aValues are in kcal/mol. ^bThe results in this work. ^cRef 29. ^dRef 41.

and the second deprotonation at bent/linear one. The first PAs of $\text{m}_a\text{-NAI}_2$ were similar to the PAs of a-NAI. Similarly, those of c-NAI₂ and t-NAI₂ were similar to the PAs of b-NAI. It results from the similarity for position of imidazolium when first deprotonation occurs at linear type for a-NAI and $\text{m}_a\text{-NAI}_2$, while at bent type for b-NAI, c-NAI₂, and t-NAI₂. Also, these tendencies are also observed for ANI₂ derivatives.

The m_a -type imidazolium derivatives generate carbene more easily than m_b -, c-, and t-type ones in that they have larger PA values resulting in more stable NHC(H⁺). Then, why do b-type monoimidazolium derivatives have higher PA than a-type ones? It is because the structure of b-type facilitate hyperconjugation^{34,35,42} against that of a-type. However, the PAs of b-type bis-imidazolium derivatives is affected by steric hindrance between methyl groups attached to adjacent imidazoliums, hyperconjugation, and instability by repulsion between neighboring lone pair electrons of the carbenes.

Thermodynamic property such as PA is useful for discussing possibility to generate carbene but it is insufficient to clarify the possibility when there is no discrepancy between comparable compounds like our systems: a-BZI and a-NAI, c-NAI₂ and t-NAI₂. Accordingly, we took a kinetic approach employing intrinsic reaction coordinate (IRC) calculation in order to establish the easiness of NHC formation. Activation energy estimated by the IRC profile could give such an information.

For all model systems in the gas phase, they immediately generated NHCs without any activation energy barrier when

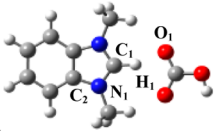


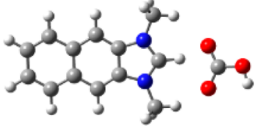
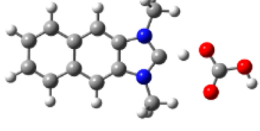
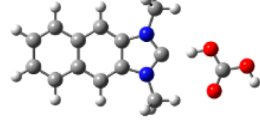
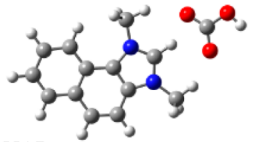


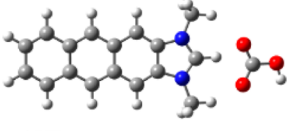
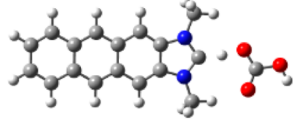
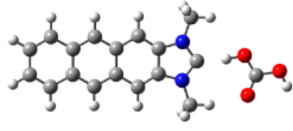
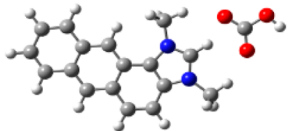
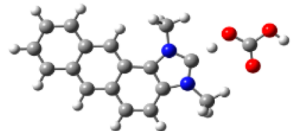
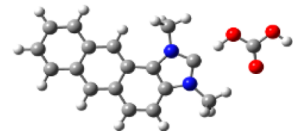
RC, [NHC(H) ⁺][B ⁻]	TS, [NHC...H...B] [‡]	PC, [NHC][HB]
 <p>a-BZI</p> <p>C₁-H₁: 1.11Å O₁-H₁: 1.71Å C₂-N₁-C₁-H₁: 179.5°</p>	 <p>C₁-H₁: 1.33Å O₁-H₁: 1.26Å C₂-N₁-C₁-H₁: 179.8°</p>	 <p>C₁-H₁: 1.64Å O₁-H₁: 1.06Å C₂-N₁-C₁-H₁: 179.7°</p>
 <p>a-NAI</p> <p>C₁-H₁: 1.11Å O₁-H₁: 1.71Å C₂-N₁-C₁-H₁: 178.4°</p>	 <p>C₁-H₁: 1.32Å O₁-H₁: 1.27Å C₂-N₁-C₁-H₁: 180.0°</p>	 <p>C₁-H₁: 1.66Å O₁-H₁: 1.05Å C₂-N₁-C₁-H₁: 179.7°</p>
 <p>b-NAI</p> <p>C₁-H₁: 1.10Å O₁-H₁: 1.82Å C₂-N₁-C₁-H₁: 178.1°</p>	 <p>C₁-H₁: 1.34Å O₁-H₁: 1.24Å C₂-N₁-C₁-H₁: 180.0°</p>	 <p>C₁-H₁: 1.62Å O₁-H₁: 1.06Å C₂-N₁-C₁-H₁: 180.0°</p>
 <p>a-ANI</p> <p>C₁-H₁: 1.11Å O₁-H₁: 1.70Å C₂-N₁-C₁-H₁: -178.5°</p>	 <p>C₁-H₁: 1.31Å O₁-H₁: 1.27Å C₂-N₁-C₁-H₁: 180.0°</p>	 <p>C₁-H₁: 1.66Å O₁-H₁: 1.05Å C₂-N₁-C₁-H₁: 180.0°</p>
 <p>b-ANI</p> <p>C₁-H₁: 1.10Å O₁-H₁: 1.82Å C₂-N₁-C₁-H₁: -179.3°</p>	 <p>C₁-H₁: 1.35Å O₁-H₁: 1.24Å C₂-N₁-C₁-H₁: -179.4°</p>	 <p>C₁-H₁: 1.62Å O₁-H₁: 1.06Å C₂-N₁-C₁-H₁: -179.6°</p>

Figure 2. Optimized structures of reactant complexes (RC), transition states (TS), and product complexes (PC) for the reaction of monoimidazolium derivatives with HCO₃⁻.

we used fluoride anion (F⁻). In particular, F⁻ enabled deprotonation for benzene moiety and methyl group of a-BZI with very small activation energy barrier of 1.88 kcal/mol. It implies that F⁻ makes it difficult to control deprotonation reaction because the anion strongly reacts with hydrogen of other functional groups as well as that of imidazolium. In order to verify solvation effect for the reaction, we additionally carried out polarizable continuum model (PCM) calculation for the same ionic species, namely, NHC precursors and F⁻. Herein, CH₃CN was used as a solvent.¹⁶

The activation energies by solvation are still too low, hence indistinguishable among them although there exists the energy barrier in transition state on the deprotonated process unlike

the situation in the gas phase. The appearance of TS results from solvation which stabilizes ionic species. In order to verify if the low activation energy barrier was caused by systemic underestimation of energetics by means of the M06-2X method, we also carried out calculations for some model systems taking solvent effect into account employing other methods, namely, B3LYP and MP2. However, the results by two methods (MP2 and B3LYP) could not support the experimental phenomenon. It was already reported that F⁻ generates NHC under CH₃CN experimentally. According to the calculation results, carbene species returned to protonated form (cationic NHC precursor) after geometry optimization using two methods. It means that carbene cannot be generated

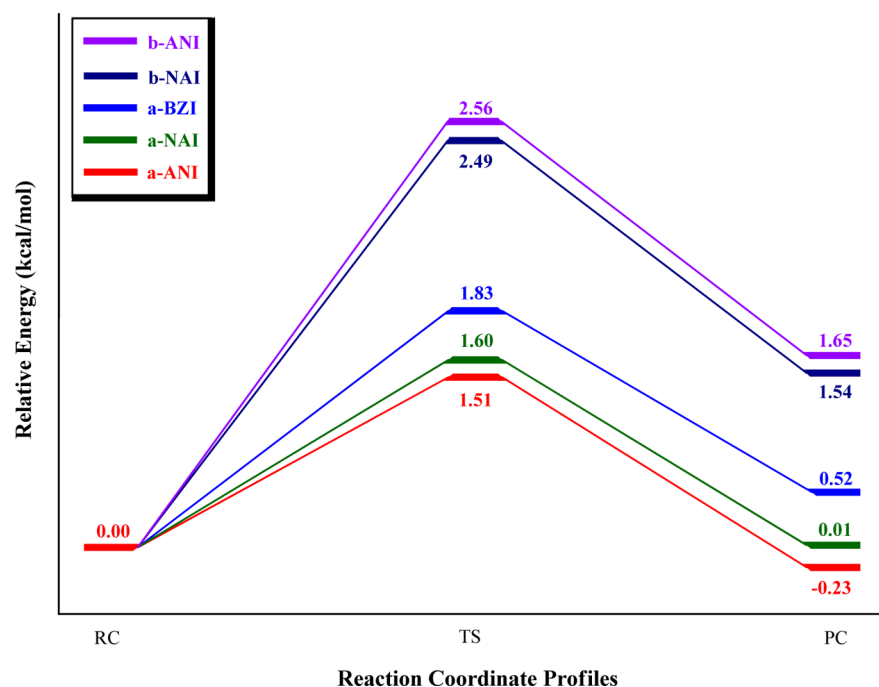


Figure 3. Activation energy for NHC precursors having monoimidazolium.

by F^- in CH_3CN when MP2 and B3LYP were used, whereas our M06-2X results demonstrated that F^- can generate NHC in CH_3CN experimentally. On the basis of the results, M06-2X method is suited for our study.

Consequently, it failed to establish the degree of easiness to generate carbenes for the NHC precursor candidates owing to the too small activation energy when we used F^- in CH_3CN , similar to leveling effect in comparing the strength of acidity/basicity. Thus, we took a weaker base HCO_3^- to generate NHC. The HCO_3^- facilitated comparison among NHC precursor candidates in both gas and solution phases.

Figure 2 illustrates optimized structures for reactant complexes (RC), transition states (TS), and product complexes (PC) for the proton transfer reaction of each NHC precursor with HCO_3^- . The bond length of O–H for the NHC precursors is independent of the size of aromatic ring and it is only dependent on the position of imidazolium: 1.70 Å for a-type NHC precursors and 1.82 Å for those of b-type, respectively. According to the tendency of bond length, a-type NHC precursors have advantage over b-type systems in the proton transfer reaction, whereas there is no severe change for other molecular constants such as bond length of C_1-H_1 or dihedral angle of $C_2-N_1-C_1-H_1$. We also looked into frequency of each species: one negative sign for complex in the transition state and all positive signs for reactants and products, respectively.

Figure 3 demonstrated activation barriers of monoimidazolium derivatives considering their IRC in transition state when proton transfer reaction occurs between each NHC precursor and hydrogen carbonate. A striking feature shown in Figure 3 is that the activation barriers of a-type are lower than those of b-type. Another feature is that the barriers are inversely proportional to the size of the aromatic moiety for the systems belonging to a-type, in that a-ANI has the smallest barrier but a-BZI has the largest one. The energy barriers of monoimidazolium derivatives are lowered in the b-ANI > b-NAI > a-BZI > a-NAI > a-ANI order, and moreover only a-ANI in

proton transfer reaction caused exothermic reaction. On the basis of the bond dissociation energies for the investigated cationic precursors, the tendency of stability for the carbenes was coincident with those of their activation energy.

Figure 4 displays optimized structures of bis-imidazolium derivatives reacting with HCO_3^- along with relevant geometrical parameters. Notable is the fact that the formation of NHC is accomplished through proton transfer between cationic NHC precursor and HCO_3^- . To compare with monoimidazolium, we added one more HCO_3^- in order to form protonated NHC salt, $[NHC(H^+)_2] \cdot 2[HCO_3^-]$, with divalent cationic bis-imidazolium. For these model systems, unlike monoimidazolium derivatives, there are two sites to produce deprotonated species. We considered both cases, however, the discrepancy between O_1-H_1 and O_2-H_2 except for mixed forms was negligible, thus we did not carry out the calculations for the opposite direction against those illustrated in Figure 4. For the mixed forms, on the other hand, we presented both cases dividing into m_a and m_b . Among the parameters, we found similarity of O_1-H_1 bond length for a- and b-types of monoimidazolium derivatives. Namely, O_1-H_1 bond length was ~ 1.60 Å for linear types, and ~ 1.90 Å for bent types. Moreover, this tendency also appeared for linear and bent position of mixed forms including the other bent forms (*c*-, and *t*-type) regardless of the number of benzene rings. The twisted geometry of *c*-NAL₂ may result from steric hindrance between adjacent methyl groups: 156.8° for dihedral angle, $N_3-C_1-N_1-C_5$. The steric hindrance disappears as the distance between methyl groups increases like in *c*-ANI₂ as shown in Figure S1. We also checked the frequency for each species: all positive frequencies for three local minima (reactant, first product, and second product) and only one negative imaginary frequency for the transition states.

Figure 5 shows the energy profiles for NHC generation from the bis-imidazolium precursors by the first and second deprotonation by IRC calculations when proton transfer reaction occurs between each NHC precursor and two

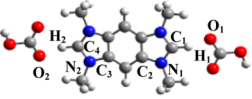
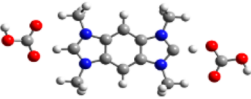
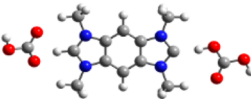
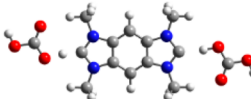
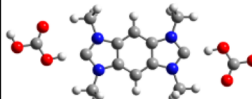
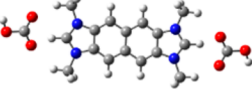
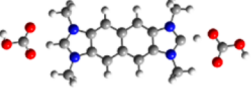
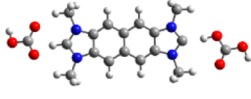
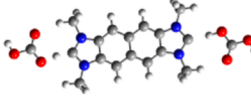
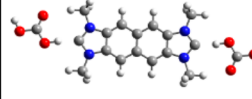
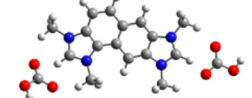
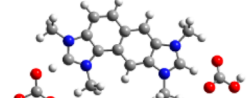
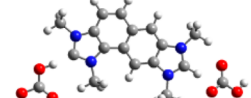
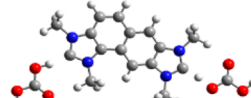
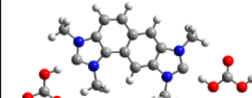
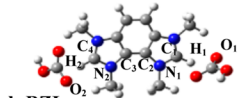
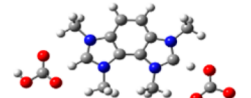
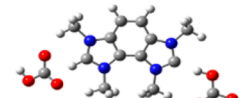
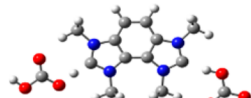
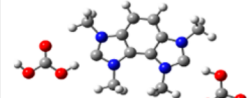
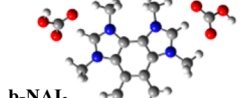
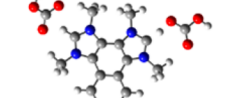
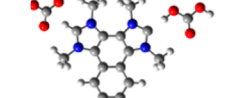
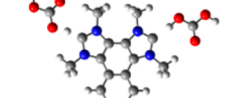
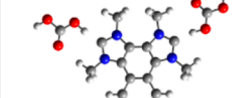
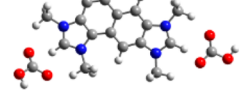
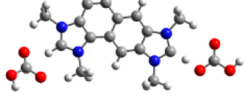
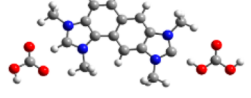
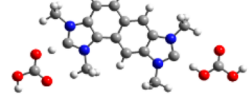
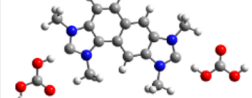
RC, [NHC(H ⁺) ₂]-2[B ⁻]	TS1, [B ⁻][NHC(H) ⁺ ...H...B] ⁺	PC1, [B ⁻][NHC(H) ⁺][HB]	TS2, [NHC...H...B] ⁺ [HB]	PC2, [NHC]-2[HB]
 <p>a-BZI₂</p> <p>C₁-H₁: 1.13Å, O₁-H₁: 1.59Å C₄-H₂: 1.13Å, O₂-H₂: 1.76Å C₂-N₁-C₁-H₁: -178.1° C₃-N₂-C₄-H₂: -177.2°</p>	 <p>C₁-H₁: 1.28Å, O₁-H₁: 1.31Å C₄-H₂: 1.12Å, O₂-H₂: 1.65Å C₂-N₁-C₁-H₁: -179.4° C₃-N₂-C₄-H₂: -177.5°</p>	 <p>C₁-H₁: 1.70Å, O₁-H₁: 1.03Å C₄-H₂: 1.09Å, O₂-H₂: 1.90Å C₂-N₁-C₁-H₁: -179.8° C₃-N₂-C₄-H₂: -176.1°</p>	 <p>C₁-H₁: 1.68Å, O₁-H₁: 1.04Å C₄-H₂: 1.31Å, O₂-H₂: 1.27Å C₂-N₁-C₁-H₁: 179.5° C₃-N₂-C₄-H₂: -179.8°</p>	 <p>C₁-H₁: 1.66Å, O₁-H₁: 1.05Å C₄-H₂: 1.66Å, O₂-H₂: 1.05Å C₂-N₁-C₁-H₁: 179.5° C₃-N₂-C₄-H₂: -179.5°</p>
 <p>a-NAI₂</p> <p>C₁-H₁: 1.13Å, O₁-H₁: 1.62Å C₄-H₂: 1.13Å, O₂-H₂: 1.62Å C₂-N₁-C₁-H₁: 177.8° C₃-N₂-C₄-H₂: 178.0°</p>	 <p>C₁-H₁: 1.29Å, O₁-H₁: 1.30Å C₄-H₂: 1.12Å, O₂-H₂: 1.65Å C₂-N₁-C₁-H₁: 179.7° C₃-N₂-C₄-H₂: 177.9°</p>	 <p>C₁-H₁: 1.69Å, O₁-H₁: 1.04Å C₄-H₂: 1.11Å, O₂-H₂: 1.70Å C₂-N₁-C₁-H₁: -179.7° C₃-N₂-C₄-H₂: 178.0°</p>	 <p>C₁-H₁: 1.68Å, O₁-H₁: 1.04Å C₄-H₂: 1.31Å, O₂-H₂: 1.27Å C₂-N₁-C₁-H₁: -179.8° C₃-N₂-C₄-H₂: 180.0°</p>	 <p>C₁-H₁: 1.67Å, O₁-H₁: 1.05Å C₄-H₂: 1.67Å, O₂-H₂: 1.05Å C₂-N₁-C₁-H₁: -179.7° C₃-N₂-C₄-H₂: 179.7°</p>
 <p>m₂-NAI₂</p> <p>C₁-H₁: 1.13Å, O₁-H₁: 1.60Å C₄-H₂: 1.09Å, O₂-H₂: 1.87Å C₂-N₁-C₁-H₁: -178.2° C₃-N₂-C₄-H₂: -176.5°</p>	 <p>C₁-H₁: 1.12Å, O₁-H₁: 1.66Å C₄-H₂: 1.31Å, O₂-H₂: 1.28Å C₂-N₁-C₁-H₁: -177.7° C₃-N₂-C₄-H₂: 179.7°</p>	 <p>C₁-H₁: 1.11Å, O₁-H₁: 1.69Å C₄-H₂: 1.67Å, O₂-H₂: 1.04Å C₂-N₁-C₁-H₁: -177.8° C₃-N₂-C₄-H₂: 179.5°</p>	 <p>C₁-H₁: 1.30Å, O₁-H₁: 1.28Å C₄-H₂: 1.66Å, O₂-H₂: 1.05Å C₂-N₁-C₁-H₁: -179.6° C₃-N₂-C₄-H₂: 179.8°</p>	 <p>C₁-H₁: 1.67Å, O₁-H₁: 1.04Å C₄-H₂: 1.64Å, O₂-H₂: 1.05Å C₂-N₁-C₁-H₁: 179.8° C₃-N₂-C₄-H₂: -179.9°</p>
 <p>b-BZI₂</p> <p>C₁-H₁: 1.09Å, O₁-H₁: 1.93Å C₄-H₂: 1.08Å, O₂-H₂: 1.98Å C₂-N₁-C₁-H₁: -175.0° C₃-N₂-C₄-H₂: -174.4°</p>	 <p>C₁-H₁: 1.28Å, O₁-H₁: 1.31Å C₄-H₂: 1.13Å, O₂-H₂: 1.63Å C₂-N₁-C₁-H₁: -179.2° C₃-N₂-C₄-H₂: -178.4°</p>	 <p>C₁-H₁: 1.70Å, O₁-H₁: 1.03Å C₄-H₂: 1.10Å, O₂-H₂: 1.75Å C₂-N₁-C₁-H₁: -178.0° C₃-N₂-C₄-H₂: -177.6°</p>	 <p>C₁-H₁: 1.68Å, O₁-H₁: 1.04Å C₄-H₂: 1.32Å, O₂-H₂: 1.26Å C₂-N₁-C₁-H₁: 179.5° C₃-N₂-C₄-H₂: 179.0°</p>	 <p>C₁-H₁: 1.66Å, O₁-H₁: 1.05Å C₄-H₂: 1.65Å, O₂-H₂: 1.05Å C₂-N₁-C₁-H₁: 179.5° C₃-N₂-C₄-H₂: 178.5°</p>
 <p>b-NAI₂</p> <p>C₁-H₁: 1.09Å, O₁-H₁: 1.91Å C₄-H₂: 1.09Å, O₂-H₂: 1.85Å C₂-N₁-C₁-H₁: -174.1° C₃-N₂-C₄-H₂: -174.4°</p>	 <p>C₁-H₁: 1.30Å, O₁-H₁: 1.29Å C₄-H₂: 1.10Å, O₂-H₂: 1.84Å C₂-N₁-C₁-H₁: -177.7° C₃-N₂-C₄-H₂: -176.7°</p>	 <p>C₁-H₁: 1.68Å, O₁-H₁: 1.04Å C₄-H₂: 1.09Å, O₂-H₂: 1.87Å C₂-N₁-C₁-H₁: -178.4° C₃-N₂-C₄-H₂: -176.8°</p>	 <p>C₁-H₁: 1.66Å, O₁-H₁: 1.05Å C₄-H₂: 1.33Å, O₂-H₂: 1.25Å C₂-N₁-C₁-H₁: 178.3° C₃-N₂-C₄-H₂: 178.3°</p>	 <p>C₁-H₁: 1.64Å, O₁-H₁: 1.05Å C₄-H₂: 1.64Å, O₂-H₂: 1.05Å C₂-N₁-C₁-H₁: 178.0° C₃-N₂-C₄-H₂: 177.9°</p>
 <p>m₁-NAI₂</p> <p>C₁-H₁: 1.13Å, O₁-H₁: 1.60Å C₄-H₂: 1.09Å, O₂-H₂: 1.87Å C₂-N₁-C₁-H₁: -178.2° C₃-N₂-C₄-H₂: -176.5°</p>	 <p>C₁-H₁: 1.28Å, O₁-H₁: 1.31Å C₄-H₂: 1.09Å, O₂-H₂: 1.86Å C₂-N₁-C₁-H₁: -179.1° C₃-N₂-C₄-H₂: -177.2°</p>	 <p>C₁-H₁: 1.70Å, O₁-H₁: 1.03Å C₄-H₂: 1.09Å, O₂-H₂: 1.93Å C₂-N₁-C₁-H₁: -179.4° C₃-N₂-C₄-H₂: -177.5°</p>	 <p>C₁-H₁: 1.68Å, O₁-H₁: 1.04Å C₄-H₂: 1.33Å, O₂-H₂: 1.25Å C₂-N₁-C₁-H₁: 179.8° C₃-N₂-C₄-H₂: -179.9°</p>	 <p>C₁-H₁: 1.67Å, O₁-H₁: 1.04Å C₄-H₂: 1.64Å, O₂-H₂: 1.05Å C₂-N₁-C₁-H₁: 179.8° C₃-N₂-C₄-H₂: -179.9°</p>

Figure 4. continued

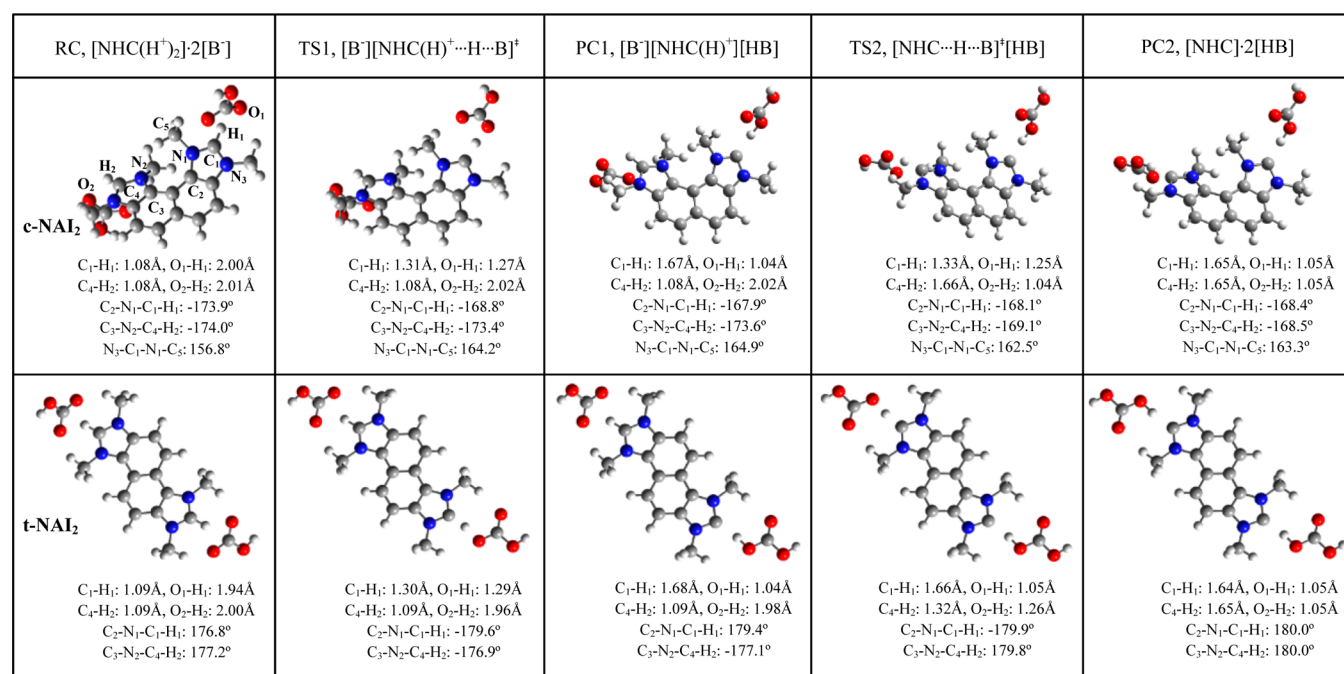


Figure 4. Optimized structures of reactant complexes (RC), transition states (TS) and product complexes (PC) for the reaction of bis-imidazolium derivatives with two HCO₃⁻. For ANI₂, they are seen in Figure S1.

hydrogen carbonates. It is remarkable that most of the first products (PC1) on proton transfer reaction are exothermic reaction comparing with monoimidazolium derivatives; only *a*-ANI is exothermic reaction in Figure 3. It demonstrated that the number of imidazolium moiety is an important factor to decrease activation barrier: 1.83 kcal/mol for *a*-BZI (in Figure 3) and 0.71 kcal/mol for *a*-BZI₂.

The position of *N*-heterocyclic moiety, in common with monoimidazolium derivatives, also has a strong influence on the activation barrier: 3.50 kcal/mol for *c*-NAI₂ and 0.73 kcal/mol for *m_b*-NAI₂. The energy barrier for each *a*-type model system was lowered by ca. 45% compared with each *b*-type model systems, for example, 0.71 kcal/mol for *a*-BZI₂ and 1.27 kcal/mol for *b*-BZI₂. The higher barrier for *b*-type is due to steric effect for neighboring imidazolium functional group.

It was clearly demonstrated that the activation energy barrier for mixed forms (*m_a*- and *m_b*-type) was lowered more effectively and the intermediate products (PC1) become more stable depending on the order of deprotonation. As seen in Figure 4, the first deprotonation for *m_b*-NAI₂ occurs in the linearly positioned imidazolium, and the geometry proximity of deprotonation site looks similar to that of *a*-NAI₂. The difference in the first activation energies between *m_b*-NAI₂ and *a*-NAI₂ is only 0.10 kcal/mol and their first dissociation energy difference is within 0.28 kcal/mol as seen in Figure 5. However, the second activation energy and dissociation for *m_b*-NAI₂ are different from those of *a*-NAI₂ because the second deprotonation occurs in the bent position unlike *a*-NAI₂.

Because of partial linear character, mixed type bis-imidazolium derivatives can produce NHC more easily than typical bent form (*b*-, *c*-, *t*-type) bis-imidazolium ones in the process of the second deprotonation. Similarly, the mixed type bis-imidazolium derivatives have higher activation energy and dissociation energy than typical *a*-type bis-imidazolium ones in the process of the second deprotonation.

Moreover, the second deprotonation reaction is exothermic for all the *a*-type bisimidazolium derivatives including *m_a*-type, while endothermic for most of typical bent form bis-imidazolium ones: *b*-NAI₂, *b*-ANI₂, *c*-NAI₂, *c*-ANI₂, and *t*-ANI₂. Among the model systems investigated in this work, *c*-NAI₂ is the highest in activation energy barrier because of its steric hindrance.

In contrast to monoimidazolium derivatives, activation barrier of bis-imidazolium derivatives increased as aromatic ring size increase. These conflicting tendency between mono- and bis-imidazolium derivatives resulted from the increment of π -electrons for monoimidazolium and relaxation of the repulsion between positive charges for bis-imidazolium derivatives, respectively. For monoimidazolium derivatives, the resonance of π -electrons enhances as the number of benzene ring increases leading to enhancement of their acidity, which lowers the activation barrier.

For bis-imidazolium derivatives, however, the activation barrier is mainly controlled by the repulsion between positive charges of two *N*-heterocyclic functional groups. Positive charges of the functional groups are distant from each other in proportion to the number of aromatic rings, which means cationic reactants become more stable as the number of aromatic ring size increases. As a result, the energy barrier increases as the number of aromatic rings increases.

We compared relative energies for the deprotonated species (free NHC) because thermodynamic stability of the resultant NHC may be crucial for practical synthesis because of the low activation energy: 0.00 kcal/mol for *a*-NAI₂, 0.19 kcal/mol for *m*-NAI₂, 9.96 kcal/mol for *b*-NAI₂, 10.39 kcal/mol for *c*-NAI₂. The tendency of relative energies for NAI₂ carbene conformers was qualitatively similar to that of corresponding activation energy barriers. According to the stability of the resultant NHCs, it is certain that *a*-type NHC conformers including mixed form are more stable than *b*-type ones. Considering the considerable deviation for relative energy among the different

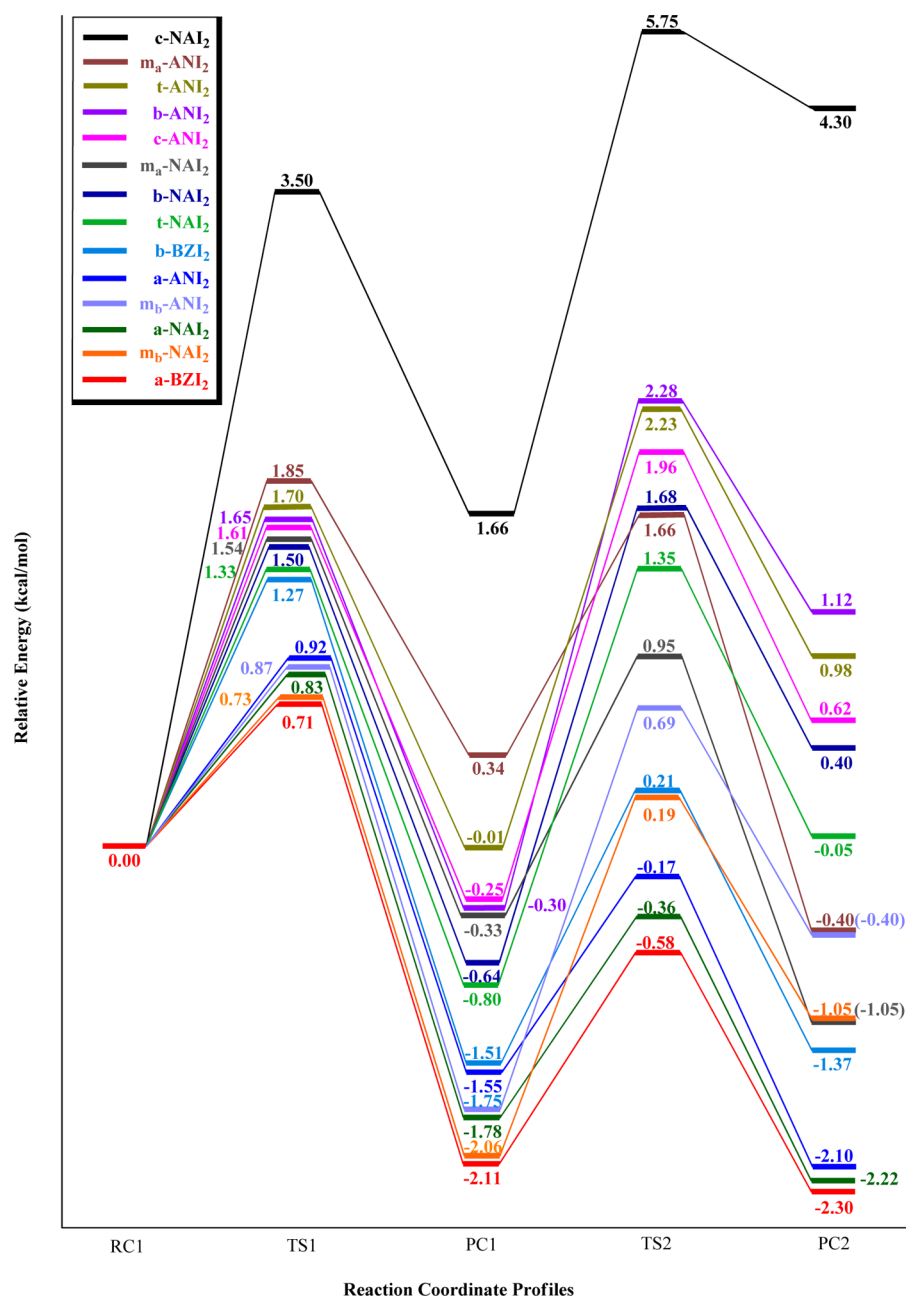


Figure 5. Energy profiles for NHC generation from the bis-imidazolium precursors by the first and second deprotonation.

carbene species, the two carbene centers have a certain interactions.

It can be considered that the difference between activation energy barriers for the model systems investigated in this work is low: 0.71 kcal/mol for a-BZI₂ and 1.27 kcal/mol for b-BZI₂. However, their relative energies between the carbene conformers can facilitate distinction for efficient NHC: 0.00 kcal/mol for a-BZI₂, 4.98 kcal/mol for b-BZI₂. From both the kinetic (activation barriers) and thermodynamic (relative stability of NHCs) aspects, it is obvious that there is correlation among the number of imidazolium functional groups, steric hindrance, and their activation energy barriers to generate free carbene.

CONCLUSIONS

We investigated the NHC precursors on geometry, proton affinity, and activation energy barrier for the proton transfer to

give NHCs by DFT calculations. Especially, we focused on the change of activation barriers as functions of conjugation length (the number of benzene ring), the number of imidazolium moiety, and the topology depending on the arrangement of imidazolium moiety. For the activation energy barrier of the model systems designed in this work, there was no coherent tendency depending on the number of benzene rings. The activation energies for the first deprotonation of the precursors fluctuated without any tendency in the following order: *c*-NAI₂ > *b*-ANI > *b*-NAI > *a*-BZI > *m_b*-ANI₂ > *b*-NAI₂ > *t*-ANI₂ > *b*-BZI₂ > *a*-ANI₂ > *m_a*-NAI₂ > *a*-BZI₂. On the other hand, the activation energies showed a remarkable dependence on the number of imidazolium moieties and their arrangements (linear, bent, mixed forms): (1) activation energies of monoimidazolium derivatives are higher than those of bis-imidazolium ones for the first deprotonation, (2) linear forms

(a- and m_a-type) have lower activation energies than bent forms (b-, c- t-, and m_b-type), and (3) steric hindrance of model system is important in that the activation energy of c-NAl₂ is the highest even though it belongs to bis-imidazolium derivatives.

The results remind us that main factors to lower activation energy barrier of the model systems are the number of imidazolium moiety, the position, and their steric hindrance in the systems. Consequently, increasing the number of imidazolium moiety and decreasing steric hindrance depending on the position of the moiety can be an effective way to lower activation energy barrier of model system. It is very important to lower the barrier in order to produce NHCs. The information given herein can provide the direction for modeling and synthesis of versatile NHC precursor spotlighted in many fields.

■ ASSOCIATED CONTENT

■ Supporting Information

Cartesian coordinates for optimized geometries, total energies of model systems for proton affinity and for activation energy barriers. This material is available free of charge via the Internet at <http://pubs.acs.org>.

■ AUTHOR INFORMATION

Corresponding Authors

*E-mail: jyoon@ewha.ac.kr.

*E-mail: jinylee@skku.edu.

Notes

The authors declare no competing financial interest.

■ ACKNOWLEDGMENTS

This work was supported by the National Research Foundation of Korea (NRF) Grant (NRF-2012K1A2B1A03000362). The authors would like to acknowledge the support from KISTI supercomputing center through the strategic support program for the supercomputing application research [No. KSC-2012-C2-73].

■ REFERENCES

- Enders, D.; Niemeier, O.; Henseler, A. *Chem. Rev.* **2007**, *107*, 5606.
- Igau, A.; Grutzmacher, H.; Baceiredo, A.; Bertrand, G. *J. Am. Chem. Soc.* **1988**, *110*, 6463.
- Bourissou, D.; Guerret, O.; Gabbai, F. P.; Bertrand, G. *Chem. Rev.* **2000**, *100*, 39.
- Igau, A.; Baceiredo, A.; Trinquier, G.; Bertrand, G. *Angew. Chem., Int. Ed.* **1989**, *28*, 621.
- Regitz, M. *Angew. Chem., Int. Ed.* **1991**, *30*, 674.
- Viciu, M. S.; Germaneau, R. F.; Navarro-Fernandez, O.; Stevens, E. D.; Nolan, S. P. *Organometallics* **2002**, *21*, 5470.
- Marion, N.; Díez-González, S.; Nolan, S. P. *Angew. Chem., Int. Ed.* **2007**, *46*, 2988.
- Dröge, T.; Glorius, F. *Angew. Chem., Int. Ed.* **2010**, *49*, 6940.
- Suresh, C. H.; Ajitha, M. J. *J. Org. Chem.* **2013**, *78*, 3918.
- Phukan, A. K.; Guha, A. K.; Sarmah, S.; Dewhurst, R. D. *J. Org. Chem.* **2013**, *78*, 11032.
- Lee, H. M.; Zeng, J. Y.; Hu, C. H.; Lee, M. T. *Inorg. Chem.* **2004**, *43*, 6822.
- Skander, M.; Retaillieu, P.; Bourrié, B.; Schio, L.; Mailliet, P.; Marinetti, A. *J. Med. Chem.* **2010**, *53*, 2146.
- Raynaud, J.; Liu, N.; Fèvre, M.; Gnanou, Y.; Taton, D. *Polym. Chem.* **2011**, *2*, 1706.
- Budagumpi, S.; Endud, S. *Organometallics* **2013**, *32*, 1537.
- Telitel, S.; Schweizer, S.; Morlet-Savary, F.; Graff, B.; Tschamber, T.; Blanchard, N.; Fouassier, J. P.; Lelli, M.; Lacôte, E.; Lalevé, J. *Macromolecules* **2013**, *46*, 43.
- Guo, Z.; Song, N. R.; Moon, J. H.; Kim, M.; Jun, E. J.; Choi, J.; Lee, J. Y.; Bielawski, C. W.; Sessler, J. L.; Yoon, J. *J. Am. Chem. Soc.* **2012**, *134*, 17846.
- Phukan, A. K.; Guha, A. K.; Sarmah, S.; Dewhurst, R. D. *J. Org. Chem.* **2013**, *78*, 1306.
- Biedermann, F.; Rauwald, U.; Cziferszky, M.; Williams, K. A.; Gann, L. D.; Guo, B. Y.; Urbach, A. R.; Bielawski, C. W.; Scherman, O. *Chem.—Eur. J.* **2010**, *16*, 13716.
- Visbal, R.; Gimeno, M. C. *Chem. Soc. Rev.* **2014**, *43*, 3551.
- Riduan, S. N.; Zhang, Y. *Dalton Trans.* **2010**, *39*, 3347.
- Zhang, Y.; Chan, J. Y. G. *Energy Environ. Sci.* **2010**, *3*, 408.
- Denning, D. M.; Falvey, D. E. *J. Org. Chem.* **2014**, *79*, 4293.
- Macqueen, P. M.; Hach, R. A.; Maclean, C. T. P.; Macquarrie, S. L. *J. Phys. Chem. C* **2014**, *118*, 5239.
- Boydston, A. J.; Vu, P. D.; Dykhno, O. L.; Chang, V.; Wyatt, A. R.; Stockett, A. S.; Ritschdorff, E. T.; Shear, J. B.; Bielawski, C. W. *J. Am. Chem. Soc.* **2008**, *130*, 3143.
- Ajitha, M. J.; Huresh, C. H. *J. Org. Chem.* **2012**, *77*, 1087.
- Wiggins, K. M.; Kerr, R. L.; Chen, Z.; Bielawski, C. W. *J. Mater. Chem.* **2010**, *20*, 5709.
- Boydston, A. J.; Pecinovsky, C. S.; Chao, S. T.; Bielawski, C. W. *J. Am. Chem. Soc.* **2007**, *129*, 14550.
- Fèvre, M.; Coupillaud, P.; Miqueu, K.; Sotiropoulos, J. M.; Vignolle, J.; Taton, D. *J. Org. Chem.* **2012**, *77*, 10135.
- Liu, M.; Chen, M.; Zhang, S.; Yang, I.; Buckley, B.; Lee, J. K. *J. Phys. Org. Chem.* **2011**, *24*, 929.
- Fèvre, M.; Pinaud, J.; Leteneur, A.; Gnanou, Y.; Vignolle, J.; Taton, D.; Miqueu, K.; Sotiropoulos, J.-M. *J. Am. Chem. Soc.* **2012**, *134*, 6776.
- Lee, C.; Yang, W.; Parr, R. G. *Phys. Rev. B: Condens. Matter Mater. Phys.* **1988**, *37*, 785.
- Becke, A. D. *J. Chem. Phys.* **1993**, *98*, 1372.
- Becke, A. D. *J. Chem. Phys.* **1993**, *98*, 5648.
- Baek, K. Y.; Hayashi, M.; Fujimura, Y.; Lin, S. H.; Kim, S. K. *J. Phys. Chem. A* **2010**, *114*, 7583.
- Baek, K. Y.; Hayashi, M.; Fujimura, Y.; Lin, S. H.; Kim, S. K. *J. Phys. Chem. A* **2011**, *115*, 7658.
- Walker, M.; Harvey, A. J. A.; Sen, A.; Dessent, C. E. H. *J. Phys. Chem. A* **2013**, *117*, 12590.
- Zhao, Y.; Ng, H. T.; Hanson, E. J. *Chem. Theory Comput.* **2009**, *5*, 2726.
- Zhao, Y.; Truhlar, D. G. *Theor. Chem. Acc.* **2008**, *120*, 215.
- Frisch, M. J.; Trucks, G. W.; Schlegel, H. B.; Scuseria, G. E.; Robb, M. A.; Cheeseman, J. R.; Scalmani, G.; Barone, V.; Mennucci, B.; Petersson, G. A.; Nakatsuji, H.; Caricato, M.; Li, X.; Hratchian, H. P.; Izmaylov, A. F.; Bloino, J.; Zheng, G.; Sonnenberg, J. L.; Hada, M.; Ehara, M.; Toyota, K.; Fukuda, R.; Hasegawa, J.; Ishida, M.; Nakajima, T.; Honda, Y.; Kitao, O.; Nakai, H.; Vreven, T.; Montgomery, J. A., Jr.; Peralta, J. E.; Ogliaro, F.; Bearpark, M.; Heyd, J. J.; Brothers, E.; Kudin, K. N.; Staroverov, V. N.; Kobayashi, R.; Normand, J.; Raghavachari, K.; Rendell, A.; Burant, J. C.; Iyengar, S. S.; Tomasi, J.; Cossi, M.; Rega, N.; Millam, N. J.; Klene, M.; Knox, J. E.; Cross, J. B.; Bakken, V.; Adamo, C.; Jaramillo, J.; Gomperts, R.; Stratmann, R. E.; Yazyev, O.; Austin, A. J.; Cammi, R.; Pomelli, C.; Ochterski, J. W.; Martin, R. L.; Morokuma, K.; Zakrzewski, V. G.; Voth, G. A.; Salvador, P.; Dannenberg, J. J.; Dapprich, S.; Daniels, A. D.; Farkas, Ö.; Foresman, J. B.; Ortiz, J. V.; Cioslowski, J.; Fox, D. J. *Gaussian 09, Revision B.01*; Gaussian, Inc.: Wallingford, CT, 2009.
- Hollóczki, O.; Kelemen, Z.; Nyulászi, L. *J. Org. Chem.* **2012**, *77*, 6014.
- Liu, M.; Yang, I.; Buckley, B.; Lee, J. K. *Org. Lett.* **2010**, *12*, 4764.
- Sahnoun, R.; Fujimura, Y.; Kabuto, K.; Takeuchi, Y.; Noyori, R. *J. Org. Chem.* **2007**, *72*, 7923.